Chinese Chemical Letters 32 (2021) 822–825

Contents lists available at ScienceDirect

Chinese Chemical Letters

journal homepage: www.elsevier.com/locate/cclet

Communication

Ion transport regulation through triblock copolymer/PET asymmetric nanochannel membrane: Model system establishment and rectification mapping

Linsen Yang[a,b], Pei Liu[a,b], Congcong Zhu[a,b], Yuanyuan Zhao[a,b], Miaomiao Yuan[c], Xiang-Yu Kong[a,*], Liping Wen[a,b], Lei Jiang[a,b]

[a] Key Laboratory of Bio-inspired Materials and Interfacial Science, Technical Institute of Physics and Chemistry, Chinese Academy of Sciences, Beijing 100190, China
[b] School of Future Technology, University of Chinese Academy of Science, Beijing 100049, China
[c] The Eighth Affiliated Hospital, Sun Yat-sen University, Shenzhen 518033, China

ARTICLE INFO

Article history:
Received 13 March 2020
Received in revised form 24 April 2020
Accepted 25 April 2020
Available online 5 May 2020

Keywords:
Nanochannel
Unidirectional rectification
Composited membrane
Ion transport
Rectification mapping

ABSTRACT

Controlling ions transport across the membrane at different pH environments is essential for the physiological process and artificial systems. Many efforts have been devoted to pH-responsive ion gating, while rarely systems can maintain the rectification in pH-changing environments. Here, a composite nanochannel system is fabricated, which shows unidirectional rectification with high performance in a wide pH range. In the system, block copolymer (BCP) and polyethylene terephthalate (PET) are employed for the amphoteric nanochannels fabrication. Based on the composite system, a model is built for the theoretical simulation. Thereafter, rectification mapping is conducted on the system, which can provide abundant information about the relations between charge distribution and ions transport properties. The proposed rectification mapping can definitely help to design new materials with special ion transport properties, such as high-performance membranes used in the salinity gradient power generation field.

Biological ion channels can control the ion inflow and outflow across the cell as nanoscale gatekeepers, which is essential to many life processes [1–3]. Due to the fragility of the natural ion channels, it is difficult to integrate them into devices [4,5]. Smart artificial nanochannels mimicking the functions including ion gating [6–8], ion rectification [9,10], and ion selectivity [11] have been a focus field due to their potential applications in pharmacy, sensing, energy, and desalination [12–21]. For example, Siwy and coworkers created a gate system for water, ionic, and neutral species by applying an electric potential across a single hydrophobic nanopore [22]. Wen *et al.* realized light-controlled ion transport through artificial channels by employing DNA technology [23]. Wang and coworkers fabricated an asymmetric heterogeneous nanowire membrane which can realize reversible ionic rectification due to the pH-regulating asymmetric wettability [24]. By employing the block copolymer, a series of heterogeneous membrane with well-controlled ionic transport were fabricated and further applied in osmotic energy harvesting [25–30]. Normally, the nanochannel geometry, surface charge polarity, charge density, and wettability are the main factors that control the mass transport properties in the nanoconfined channels [31–34]. By regulating the above-mentioned factors, artificial nanochannel with desired mass transport properties, such as ionic diode, can be constructed [35,36]. Normally, the ion rectification direction and rectifying performance of the fabricated nanochannels will change along with the external pH stimuli and cannot maintain the desired rectification properties, which limits their practical applications, such as osmotic energy harvesting. Yet, rare details of regulating pH-sensitivity and mapping the rectification of the systems have been stated.

Here, we proposed a facile strategy for making artificial ion channels that show unidirectional rectification in a wide pH range from acidic to basic environment by combining triblock copolymer and nanoporous PET nanochannels. Briefly, the membrane was prepared by casting the BCP membrane, poly(styrene-*b*-*tert*-butyl methacrylate-*b*-2-vinylpyridine (PS-*b*-PtBuMA-*b*-P2VP), onto a PET membrane with conical nanochannels (10^6 cm^{-2}) produced by ion-track etching protocol (Fig. S1 in Supporting information) [37]. The system shows unidirectional ion rectification effect in a broad pH range from 3 to 11 due to the synergistic effects of the

* Corresponding author.
E-mail address: kongxiangyu@mail.ipc.ac.cn (X.-Y. Kong).

https://doi.org/10.1016/j.cclet.2020.04.047
1001-8417/

surface charge distribution and the multilevel channel geometry, and the maximum rectification ratio can achieve 200. As the BCP in our system contains multiple blocks with optional functional groups (pH sensitive) and holds well performance in film building [38], it is suitable to be used as a model system for exploring the influencefactors on ionic rectification. Based on this model system, the rectification mapping is carried out for the first time by employing theoretical simulation, which provides details on how the charge distribution and channel geometry affect the ion transport. The proposed membrane material shows broad application potential in salinity gradient power generation, and this work can provide guidance for materials designing used in energy harvesting and separation fields.

As shown in Fig. 1, the PtBuMA block in the BCP can be hydrolyzed to produce carboxyl group, which can respond to the solution pH changes. Before the hydrolysis, the BCP membrane can be positively charged or neutral in certain pH range due to the pH sensitive P2VP group. As the pK_a of copolymers in nanoconfined environment variated from the bulk value [32], several pH values are chosen to test the system. Thereafter, the hydrolysis reaction was conducted to make the BCP membrane be negatively charged in basic solution due to the produced carboxyl groups. In the meantime, the wettability of the BCP part of the membrane is also investigated with the contact angle (CA) measurement (Fig. S3 in Supporting information). The BCP membrane becomes more hydrophilic as the CA changed from 84.04° ± 1.79° to 41.58° ± 2.90° after the hydrolysis reaction. Thus, the proposed system can be used as a prototype to investigate how the different charged states of the BCP and PET nanochannels, respectively, affect the ion transport cross the membrane, which helps to better design the desired system with special ion transport properties. To better illustrate the rectification properties of the system, a rectification factor (f_{rec}), which is similar to that in Azzaroni's paper [39], is defined. The defined f_{rec} can be calculated according to the following equation (Eq. 1a):

$$f_{rec} = \begin{cases} \left|\frac{I_{+2\ V}}{I_{-2\ V}}\right| when,\ |I_{+2\ V}| \geq |I_{-2\ V}| \\ -\left|\frac{I_{-2\ V}}{I_{+2\ V}}\right| when,\ |I_{+2\ V}| < |I_{-2\ V}| \end{cases} \quad (1)$$

where f_{rec}, $I_{+2\,V}$ and $I_{-2\,V}$ are the rectification factor, current measured at +2 V, and current measured at −2 V, respectively. In the measurement, the anode and cathode electrode are placed at the PET and BCP side, respectively (Fig. S4 in Supporting information). In this way, a standard parameter (f_{rec}) is built for evaluating all the ion transport properties in the nanochannel system.

The ionic transport properties of our system are investigated by current-voltage (I–V) measurement. The as-prepared PET nanochannel membrane has a negative f_{rec} (Fig. S5a in Supporting information) and the composite membrane holds a positive f_{rec} after the BCP membrane casting (Fig. S5b in Supporting information). Besides, the composited membrane shows a nonlinear decrease along with the solution concentration decrease indicating a charge-governed ion transport in the system (Fig. S5c in Supporting information). Thereafter, the I–V curves of the composited membrane after hydrolysis at different pH values were investigated (Fig. 2a). All the curves show the same directional rectification behaviours. The detailed changes of the currents at negative bias are shown in Fig. S6 (Supporting information). Rectification factors at different pH conditions are presented in Fig. 2b. According to the Eq. (1), all the f_{rec} are calculated to be positive. In our testing system, the positive f_{rec} means the ions accumulated in the channels at +2 V bias and depleted at -2 V bias; and *vice versa* [40]. All the f_{rec} are bigger than 50 and the maximum value can achieve 200, showing the high ionic regulation performance. This is mainly because of the high surface charge density brought by the two parts of the composite membrane and the multilevel asymmetry brought by the PET part. For the sake of discussion, the system is simplified to a funnel shaped nanochannel according to the characterization of the composite membrane. The states of the system correspond to the ion transport at different pH can be divided to three types (type I, II and III in Fig. 2c). In the composited membrane, the BCP part and the PET part are in different charged states (charge polarity and charge density) along with the pH changes. Type I shows the charge distribution of the system in pH 2.89, and the composited membrane showed a positive-neutral (BCP-PET) charged state. Here, the neutral PET also plays an essential role in maintaining the rectification of the system, and the system is unlike the cylinder positive charged nanochannel, which shows no rectification [41]. The f_{rec} reaches the highest value (~206) in the pH 4.56 solution, and the charge distribution of the system (type II) is in a

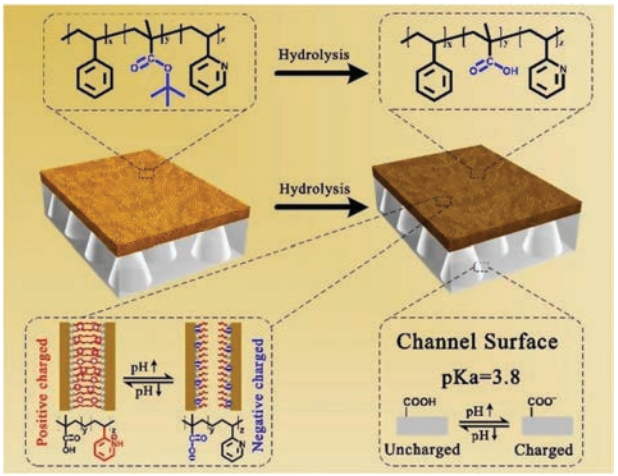

Fig. 1. The hydrolysis reaction of the composited membrane. The carboxyl groups can be produced in the *t*BuMA blocks through the hydrolysis reaction, which can be seen in the top line. After the hydrolysis reaction, the carboxyl groups and pyridyl groups (BCP part) and the carboxyl groups (PET part) can be charged or uncharged along with the pH changes, respectively.

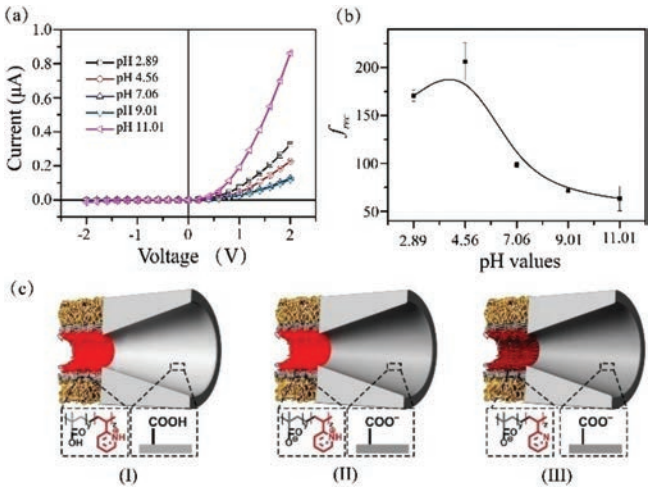

Fig. 2. Unidirectional rectification properties of the composite membrane at different pH conditions. (a) I–V curves of the composite membrane in 10 mmol/L KCl at different pH values with sweeping voltage from −2 V to 2 V. In the measurement, the anode is placed at PET side and the cathode is placed at BCP side. (b) The corresponding rectification ratios in (a). The solid line is a guide to the eye. (c) Charge distribution of the system at different pH conditions. Type I corresponds to the system at pH 2.89; Type II corresponds to the system at pH 4.56; Type III presents the charge distribution of the composite membrane at pH 7.06, 9.01 and 11.01.

positive-negative (BCP-PET) state. The high f_{rec} in this condition can ascribe to the charge and geometry asymmetry [42,43]. When the system was tested in solution with pH 7.06, 9.01 and 11.01, the system is in a negative-negative (BCP-PET) charged state (type III). This is not the situation in cylinder or conical nanochannels, which shows f_{rec} of 1 or negative value, respectively. Both the charging states and geometry could affect the rectification of the system. Also, the ionic transport properties of bare PET nanochannels and composited membrane before hydrolysis reaction were studied (detailed in Fig. S7 in Supporting information). Specially, the composited membrane before hydrolysis tested in solution at pH 9.01 also shows a positive f_{rec} value, which is in the charged state of neutral-negative (BCP-PET). Therefore, a relative completed set of charged states of the funnel nanochannel is constructed, and it is worth investigating the details of the ionic transport of all the above-mentioned charged states.

To dig into the details of the ionic transport properties of our system, numerical simulation based on Poisson–Nernst–Planck (PNP) equations was employed (Fig. S8 in Supporting information) [44,45]. Through the simulation, the detailed relations between the ionic transport and the system's characterization, such as geometry, charge polarity, and charge density, could be revealed. In Figs. 3a and b, the currents at +2 V and -2 V voltage bias with different charge distribution in BCP and PET nanochannels are presented, respectively. Besides, the concentration profiles of the K^+ and Cl^- at different charged conditions which are corresponded to the different pH solutions are showed in Fig. S9 (Supporting information). By combining the data in Figs. 3a and b, the rectification ratio distribution of the system is mapped in Fig. 3c. In our model, only the factors of the charge distribution and geometry, which will largely affect the ion transport performance of the system, are considered. Fortunately, most of our experimental results can be found in the constructed rectification mapping surface. Besides, from Fig. 3, we can get some laws between the ionic transport and the system's charged status. First, the $I_{+2\,V}$ has the biggest value (Fig. 3a) when the σ_{BCP} and σ_{PET} are 0.07 C/m^2 and -0.12 C/m^2, respectively. Along with the small $|I_{-2\,V}|$ (Fig. 3b), the big rectification factor can be gained (Fig. 3c), which is the similar situation with the experiment measured at pH 4.56 (Fig. 2b). In the meantime, the $I_{-2\,V}$ has the biggest absolute value (Fig. 3b) when the σ_{BCP} and σ_{PET} are −0.07 C/m^2 and 0.00 C/m^2, respectively. These results show that the desired current can be obtained at suitable charge distribution. Then, the ionic transport properties of the system with a neutral PET part are studied. Along with the σ_{BCP} changing from negative to positive, $|I_{+2\,V}|$ increase and $|I_{-2\,V}|$ decrease, respectively. As a result, the rectification ratio in Fig. 3c shows a symmetric pattern along with the σ_{BCP} changing, which means that the ionic transport is determined by the σ_{BCP} parameter. It does show rectification when σ_{BCP} is not zero, which is not like the situation in cylinder nanochannel [41]. So, the conical part of the funnel nanochannel is essential to its ionic transport property. On the contrary, when σ_{BCP} is zero, the funnel nanochannel shows positive f_{rec}, where an ion accumulation and depletion zone are formed in the channels at +2 V and −2 V voltage bias (Fig. S8 in Supporting information), respectively [46]. Thus, the result of our experiment conducted at pH 2.89 (Fig. 3b) can be explained. Normally, the conical nanochannel shows a negative f_{rec} due to the negative carboxyl groups. Here, by adding a section of neutral nanochannel, the ionic transport can be tuned to the opposite direction, showing that the ionic transport of the nanochannel is a comprehensive result of different factors. Thirdly, Fig. 3c shows that in the region with negative σ_{BCP} and σ_{PET}, which is the situation of the system in pH 7.06, 9.01, and 11.01 solutions, all the f_{rec} are relatively small. While in the neighbour zone with positive σ_{BCP} and negative σ_{PET}, all the f_{rec} are relatively big. Apart from the geometry, the opposite charge polarity can render the significant rectification phenomenon in the system, which is an effective way to increase the performance of the nanofluidics [33,34].

For further investigating how the ionic transport changes along with the charge status of the nanochannels, the contour plot of the rectification factor was presented (Fig. 4a). In Fig. 4a, it could be clearly seen the f_{rec} changes from the 'flat' region to the 'rough' region with big rectification factors. It is worth noting that the region fenced by the lines tagged '1.0' and '−1.0' is actually a 'dead' region which is a result of our definition of 'f_{rec}'. According to our definition, f_{rec} can be in the following three conditions: (1) equals to 1 (line with tag 1.0 in Fig. 4a), which shows no rectification; (2) bigger than 1 (right side of the '1.0' line in Fig. 4a), which shows bigger $|I_{+2\,V}|$; (3) smaller than −1 (left side of the '−1.0' line in Fig. 4a), which shows bigger $|I_{-2\,V}|$. Interestingly, the boundaries which divide the rectification map into two main regions is not overlapped with the zero line (black dash line in Fig. 4b). For understanding the detailed transition of the f_{rec} from positive to negative, the refined charge density is applied to solve the PNP equation (Numerical simulation in Supporting information) and a fine contour plot is obtained (Fig. 4b). In Fig. 4b, the rectification ratio can be equal to 1 when the σ_{BCP} and σ_{PET} are both negative with about -0.10 C/m^2 and -0.07 C/m^2, respectively. Our results are not the same with Azzaroni's report [30], where negative rectification means a negative surface charge and vice versa. The difference can be attributed to the different geometry which is also an important factor in ionic transport of the nanochannels. In the region where is fenced by the '1.00' line, black dash line, and parts of the 'σ_{BCP}' and 'σ_{PET}' axis, even both the BCP and PET nanochannels are negative charged, the positive f_{rec} can be still reached. Our ion transport experiments with pH 7.06, 9.01, and 11.01 just confirmed the above-mentioned situation. The BCP part with few —COOH groups holds low negative charges and the PET part are fully deprotonated. The findings present great potential in new nanofluidic membrane designing. For example, the reported

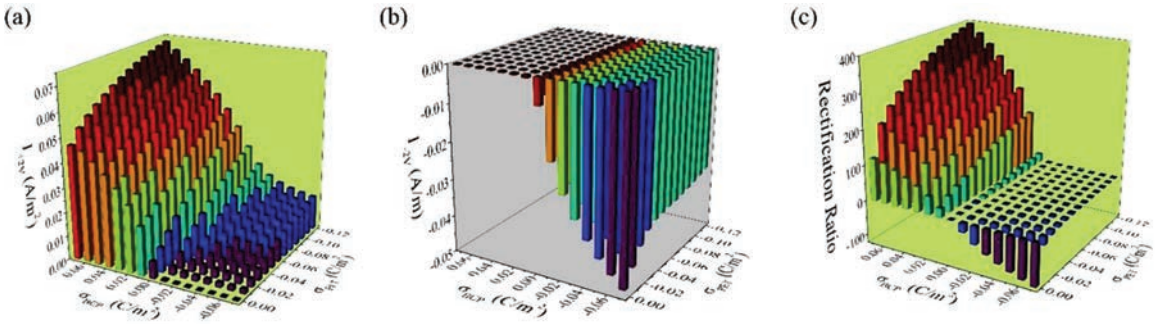

Fig. 3. Simulated currents at (a) +2 V and (b) −2 V bias with different charge density in BCP and PET nanochannels. The rectification ratio mapping (c) of the composited membrane with different charge distribution derived from (a) and (b).

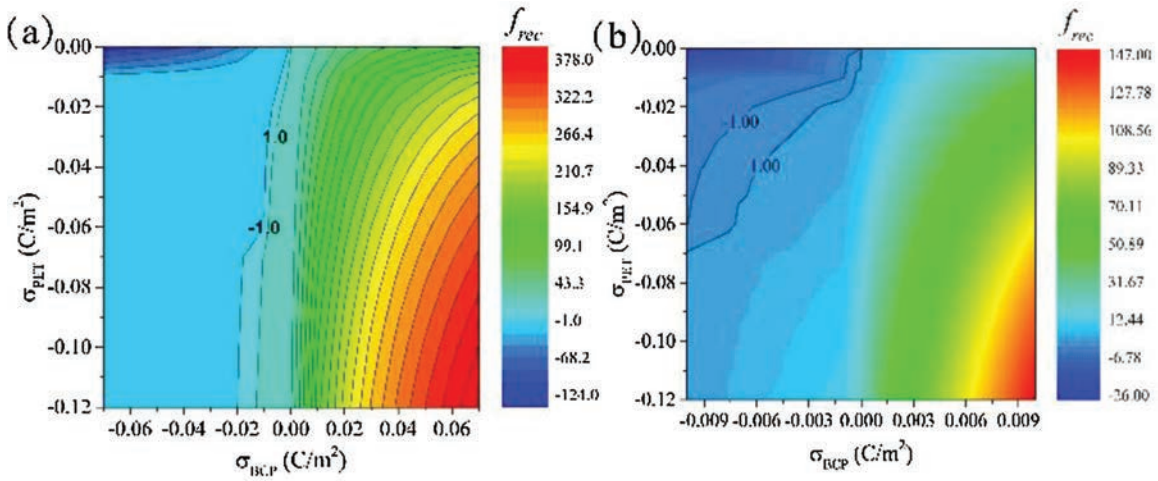

Fig. 4. Contour plot of the rectification mapping (a) Image of the different charging states of the system. (b) Image with refined BCP charge density changes.

heterogeneous membrane for osmotic energy harvest mainly worked in the pH of 4.3 [20], to maintain the opposite charge distribution. As the pH 4.3 is not suitable for the practical application, the materials work well in near neutral condition are needed to be developed. Our results point out that the opposite charge polarity for reaching positive f_{rec} in heterogeneous nanochannels [18,20] is not necessary, which can also be reached with all negative charged nanochannels.

In summary, we conducted experimental and theoretical studies on the ion transport of a composited membrane, which show positive f_{rec} in a wide pH range from acidic to basic environment. The pH responsive groups in BCP and PET along with the geometry endow the membrane with unidirectional rectification. Theoretical simulation based on PNP equation is conducted for the rectification mapping, which is devoted to better understanding the detailed ion transport. The proposed system turns out locating in the positive f_{rec} region. Specifically, it is found that even both the BCP and PET nanochannels are negative, the positive f_{rec} can be still reached. Furthermore, the rectification mapping with different charge distribution in funnel nanochannel could be used for the guidance of membrane designing in various pH conditions, showing great potential in energy harvesting and separation fields.

Declaration of competing interest

The authors declare that they have no known competing financial interests or personal relationships that could have appeared to influence the work reported in this paper.

Acknowledgments

This work was financially supported by the Beijing Natural Science Foundation (No. 2194088) and the National Natural Science Foundation of China (Nos. 21905287, 21625303, 51673206, 21988102, 81972488, 81701836).

Appendix A. Supplementary data

Supplementary material related to this article can be found, in the online version, at doi:https://doi.org/10.1016/j.cclet.2020.04.047.

References

[1] D.A. Doyle, J.M. Cabral, R.A. Pfuetzner, et al., Science 280 (1998) 69–77.
[2] J.A. Wemmie, R.J. Taugher, C.J. Kreple, Nat. Rev. Neurosci. 14 (2013) 461–471.
[3] X. Zhang, L. Jiang, Nano Res. 12 (2019) 1219–1221.
[4] S.W. Kowalczyk, T.R. Blosser, C. Dekker, Trends Biotechnol. 29 (2011) 607–614.
[5] L. Wen, L. Jiang, Sci. Rev. 1 (2014) 144–156.
[6] G. Xie, K. Xiao, Z. Zhang, et al., Angew. Chem. Int. Ed. 54 (2015) 13664–13668.
[7] H. Zhang, Y. Tian, L. Jiang, Chem. Commun. 49 (2013) 10048–10063.
[8] X. Hou, Adv. Mater. 28 (2016) 7049–7064.
[9] K. Pal Singh, K. Kumari, M. Kumar, Appl. Phys. Lett. 99 (2011) 113103.
[10] M. Wang, H. Meng, D. Wang, et al., Adv. Mater. 31 (2019) e1805130.
[11] Z. Zhang, X.Y. Kong, G. Xie, et al., Sci. Adv. 2 (2016) e1600689.
[12] X. Huang, L. Xie, X. Lin, B. Su, Anal. Chem. 89 (2017) 945–951.
[13] E.T. Lam, A. Hastie, C. Lin, et al., Nat. Biotechnol. 30 (2012) 771.
[14] S. Lu, D. Wang, S.P. Jiang, et al., Adv. Mater. 22 (2010) 971–976.
[15] J. Abraham, K.S. Vasu, C.D. Williams, et al., Nat. Nanotech. 12 (2017) 546.
[16] W. Xin, Z. Zhang, X. Huang, et al., Nat. Commun. 10 (2019) 1–10.
[17] Y. Tang, L. Cao, K. Zhan, et al., Sens. Actuators B: Chem. 286 (2019) 315–320.
[18] X. Hou, Z.S. Siwy, M. Ulbricht, Small 358 (2018) 206–210.
[19] Y. Zhu, K. Zhan, X. Hou, ACS Nano 12 (2018) 908–911.
[20] S. Chen, Y. Tang, K. Zhan, D. Sun, X. Hou, Nano Today 20 (2018) 84–100.
[21] X. Hou, Adv. Mater. 28 (2016) 7049–7064.
[22] M.R. Powell, L. Cleary, M. Davenport, K.J. Shea, Z.S. Siwy, Nat. Nanotech. 6 (2011) 798–802.
[23] P. Li, G. Xie, X.Y. Kong, et al., Angew. Chem. Int. Ed. 55 (2016) 15637–15641.
[24] J. Zhang, Y. Yang, Z. Zhang, et al., Adv. Mater. 26 (2014) 1071–1075.
[25] J. Zhang, Y. Yang, Z. Zhang, P. Wang, X. Wang, Adv. Mater. 26 (2014) 1071–1075.
[26] X. Sui, Z. Zhang, C. Li, et al., ACS Appl. Mater. Interfaces 11 (2018) 23815–23821.
[27] Z. Zhang, X.-Y. Kong, K. Xiao, et al., J. Am. Chem. Soc. 137 (2015) 14765–14772.
[28] Z. Zhang, X. Sui, P. Li, et al., J. Am. Chem. Soc. 139 (2017) 8905–8914.
[29] G. Xie, L. Wen, L. Jiang, Nano Res. 9 (2016) 59–71.
[30] Y. Zhu, K. Zhan, X. Hou, ACS Nano 12 (2018) 908–911.
[31] P.Y. Apel, I.V. Blonskaya, O.L. Orelovitch, P. Ramirez, B.A. Sartowska, Nanotechnology 22 (2011) 175302.
[32] M. Tagliazucchi, O. Azzaroni, I. Szleifer, J. Am. Chem. Soc. 132 (2010) 12404–12411.
[33] W. Zhang, Z. Meng, J. Zhai, L. Heng, Chem. Commun. 50 (2014) 3552–3555.
[34] X. Zhang, F. Zhang, F. Zhu, X. Zhang, H. Li, ACS Appl. Bio. Mater. 2 (2019) 3607–3612.
[35] K. Xiao, L. Chen, Z. Zhang, et al., Angew. Chem. Int. Ed. 56 (2017) 8168–8172.
[36] Q. Sheng, Y. Xie, J. Li, X. Wang, J. Xue, Chem. Commun. 53 (2017) 6125–6127.
[37] P. Li, X.Y. Kong, G. Xie, et al., Small 12 (2016) 1854–1858.
[38] S. Ludwigs, A. Böker, A. Voronov, et al., Nat. Mater. 2 (2003) 744–747.
[39] G. Pérez-Mitta, W.A. Marmisollé, C. Trautmann, M.E. Toimil-Molares, O. Azzaroni, Adv. Mater. 29 (2017) 1700972.
[40] H. Daiguji, Y. Oka, K. Shirono, Nano Lett. 5 (2005) 2274–2280.
[41] B. Yameen, M. Ali, R. Neumann, et al., Nano Lett. 9 (2009) 2788–2793.
[42] I. Vlassiouk, Z.S. Siwy, Nano Lett. 7 (2007) 552–556.
[43] W. Guo, Y. Tian, L. Jiang, Acc. Chem. Res. 46 (2013) 2834–2846.
[44] H.S. White, A. Bund, Langmuir 24 (2008) 2212–2218.
[45] W.-J. Lan, D.A. Holden, H.S. White, J. Am. Chem. Soc. 133 (2011) 13300–13303.
[46] K. Xiao, G. Xie, Z. Zhang, et al., Adv. Mater. 28 (2016) 3345–3350.